

# Studying the possibility of hyperon reconstruction in the BM@N experiment at the NICA complex

Made by:

Barak R.

Supervised by:

Merts S.P.

JINR Association of  
Young Scientists and  
Specialists Conference  
"Alushta-2023", 4–11 Jun  
2023

# Introduction

- Collisions of heavy relativistic ions allow us to study nuclear matter at extreme density and temperature.
- At sufficiently high temperature and energy density, the so-called Quark-Gluon Plasma (QGP) is formed [1]:
  - Hyperon formation.
- Theoretical models offer different descriptions [2],[3]:
  - New experimental data is needed for clarification.

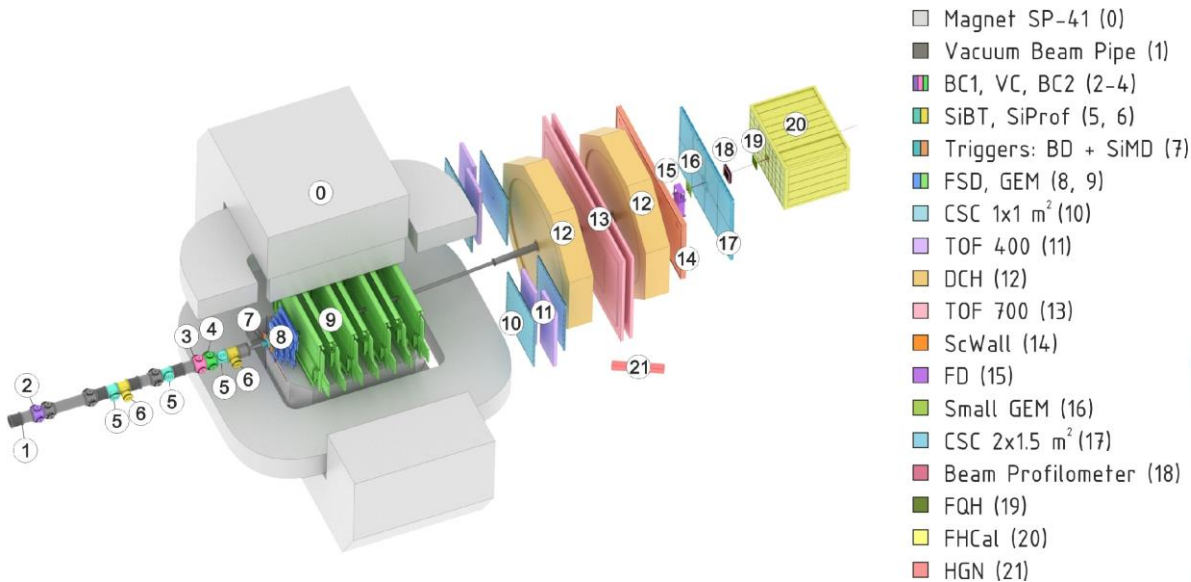
[1] Kapishin.M, “Studies of baryonic matter at the BM@N experiment (JINR).” Nuclear Physics A 982 (2019) 967–970.

[2] J. A. et al Nucl. Phys., vol. A 757, pp. 102–183, 2005.

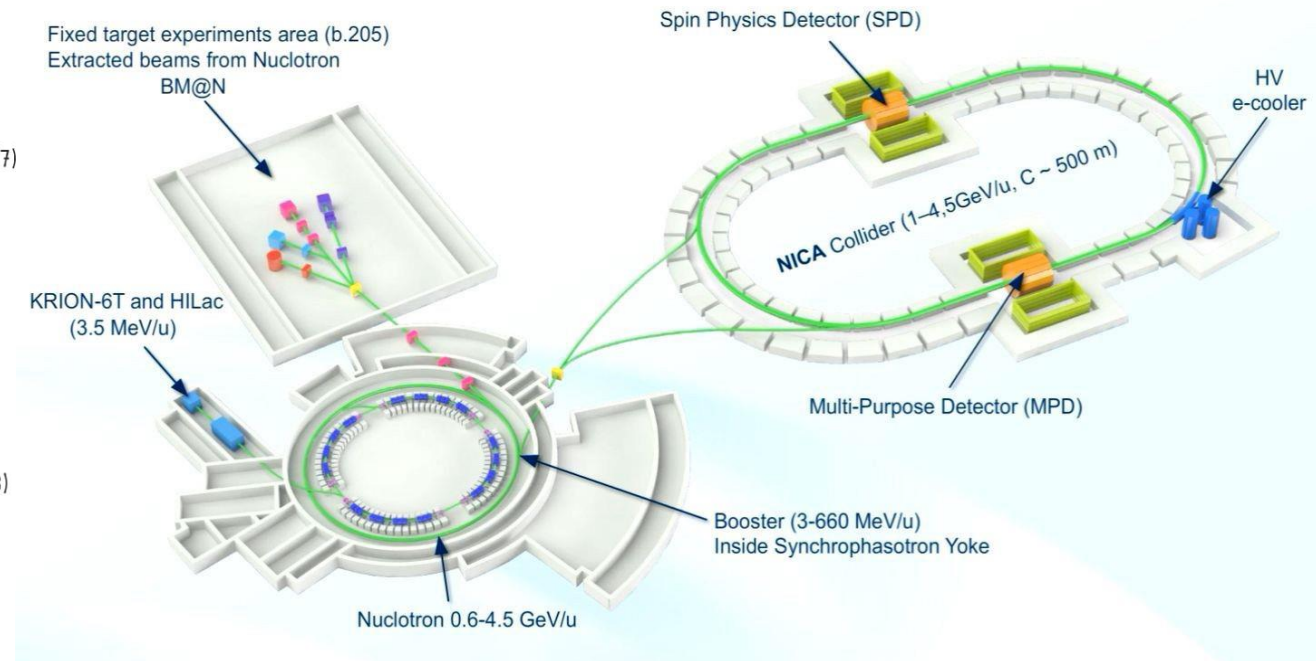
[3] K. A. et al Nucl. Phys., vol. A 757, pp. 184–283, 2005.

# BM@N experiment at the NICA complex

- Collisions of elementary particles and ions with a stationary target at energies up to 4 GeV per nucleon.



Experimental setup of BM@N



NICA accelerator complex

# Goal of the work

Search for hyperons in the data of the BM@N experiment.

## Tasks

- Modelling and reconstruction of data for analysis.
- Development and implementation of a hyperon reconstruction algorithm in bmnroot.
- Determination of the sources of background increment in the mass distribution.
- Investigation of the influence of background sources on the quality of reconstruction.

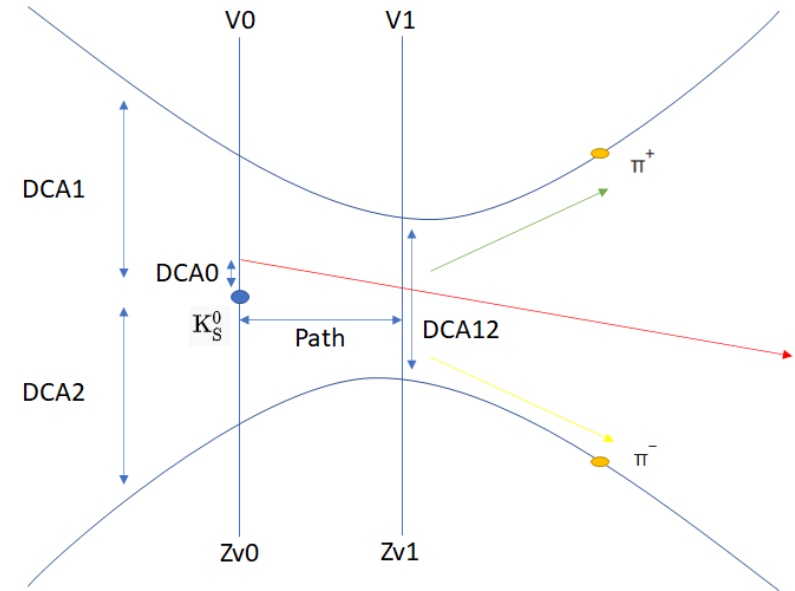
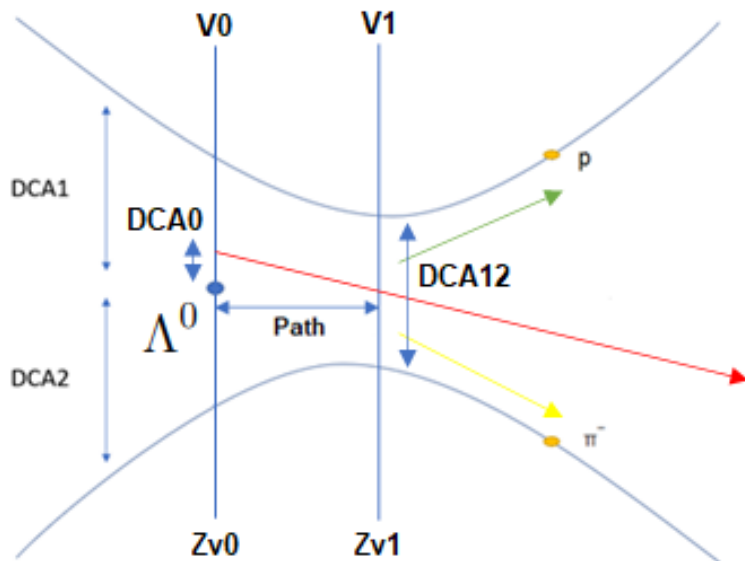
# Data

- Data obtained from the Monte Carlo generator DCMSMM [4] was used for the analysis. 100,000 events were simulated and reconstructed.

[4] Baznat M., Botvina A., Musulmanbekov G., Toneev V., Zhezher V. Monte-Carlo Generator of Heavy Ion Collisions DCM-SMM, Physics of Particles and Nuclei Letters 17, 3, 303-324 (2020)

# Data processing

- Algorithms were developed and implemented to enable the search for the trajectories of lambda hyperons along the decay channel into a proton and negative pi-meson and short-lived neutral kaons along the decay channel into positive and negative pi-mesons:
  - Sorting of pairs of particles with different signs.
  - Calculating the invariant mass.
  - Imposing a number of geometric restrictions on the parameters of each pair.



# Sources of background increment

- Blurring of the beam

- In the least realistic case, the beam is assumed to be point like. In reality, there is beam blurring in the transverse plane, as well as a small spread in angle.

- SiMD, BD

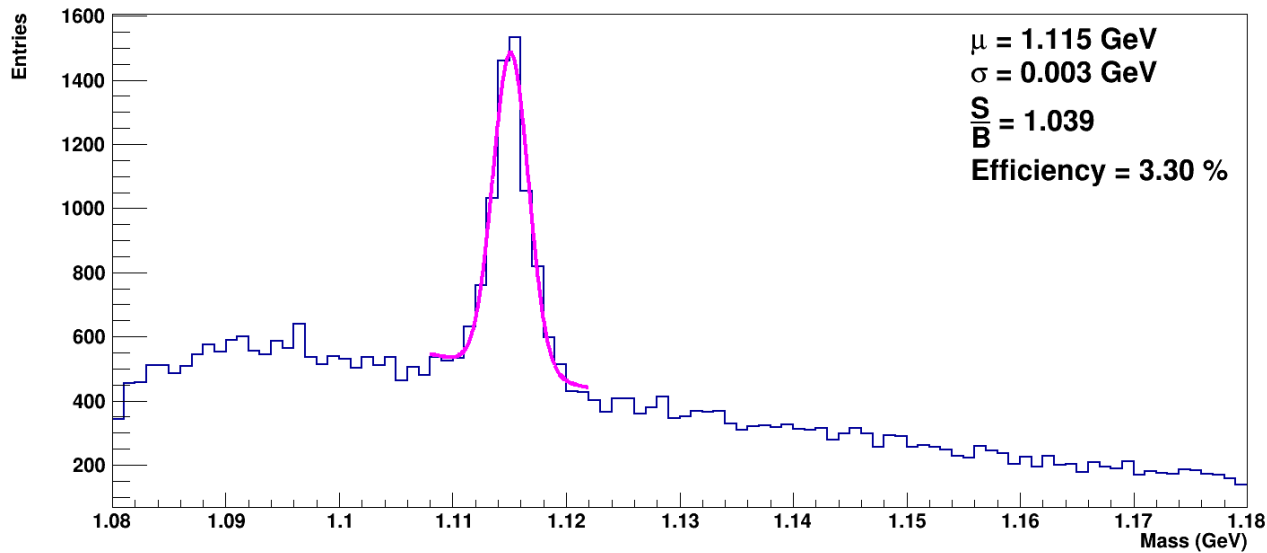
- The production of secondary particles and, as a consequence, an increase in the background in the mass distribution of lambda hyperons, can be affected by the presence of the substance of trigger detectors located after the target and before the track detectors.

- Target

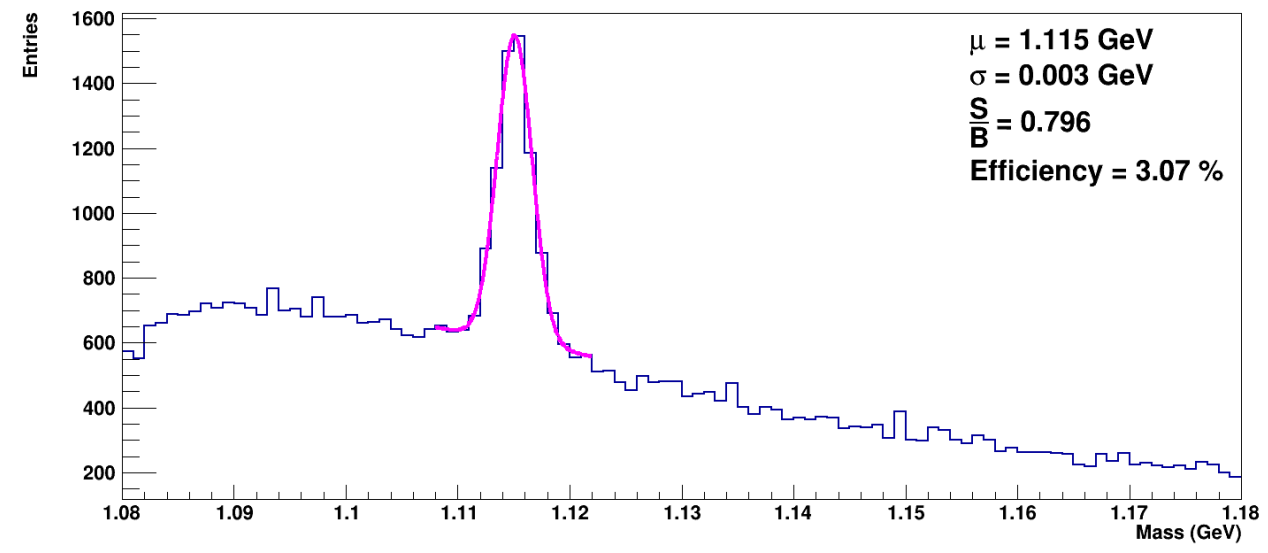
- Since the target is an extended object, in addition to the primary interaction of the beam with the target, there will be interactions of secondary particles with the target nuclei. This might also be a source of the background increment in the mass spectra.

# Results

## Lambda hyperons



Ideal case



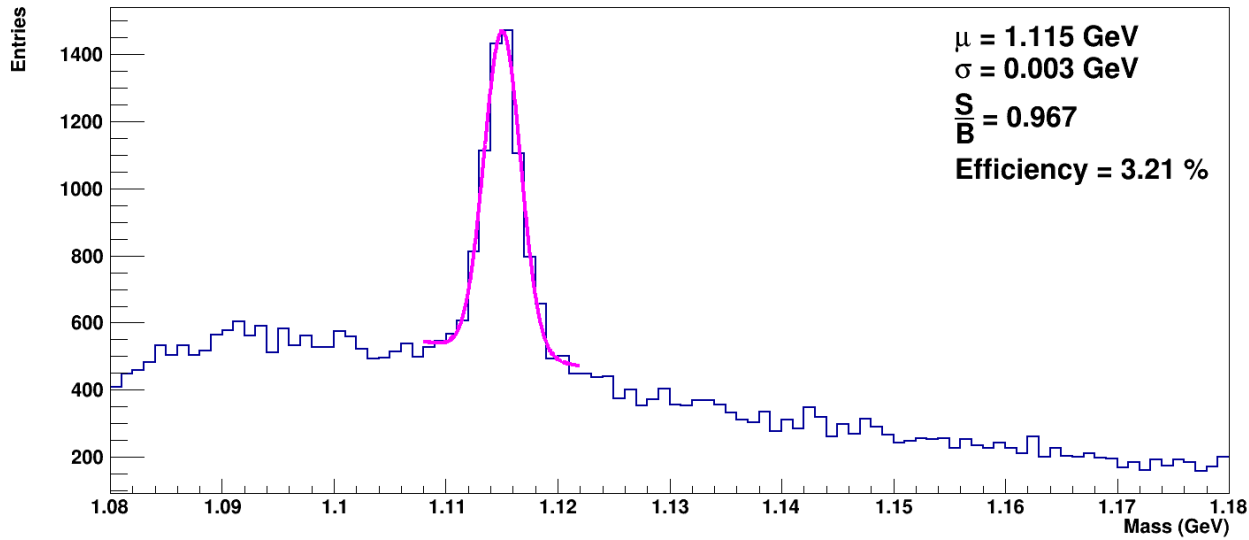
SiMD, BD, target and beam blurring

- Cuts

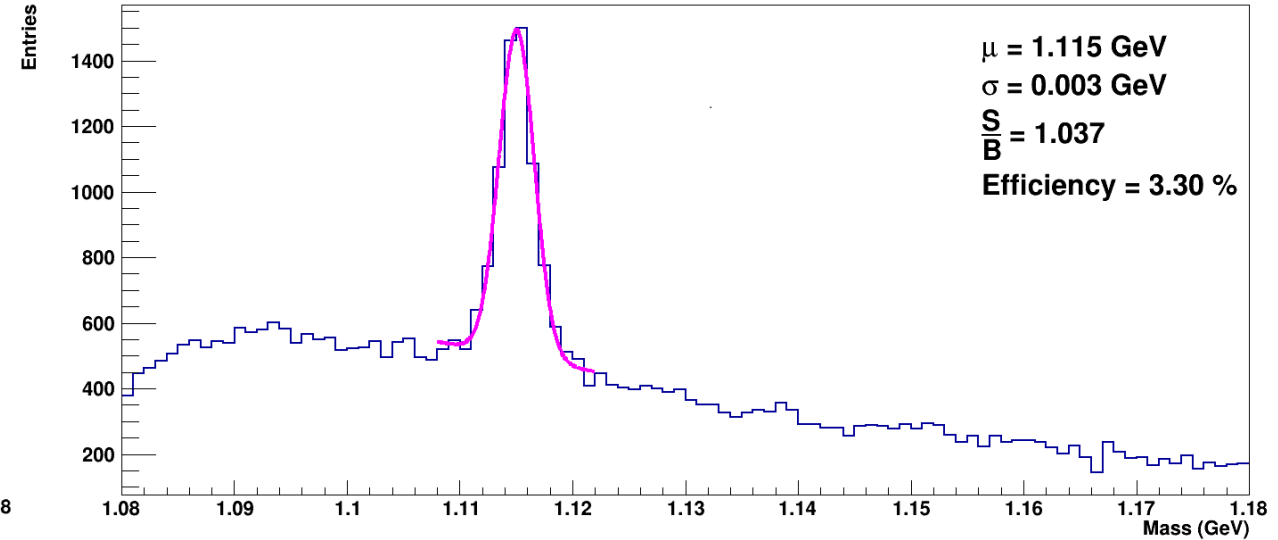
- $3.0 < \text{path} < 20$
- $0.0 < \text{DCA12} < 0.4$
- $0.0 < \text{DCA0} < 0.2$
- $0.1 < \text{DCA1} < 3.0$
- $0.3 < \text{DCA2} < 3.0$

# Results

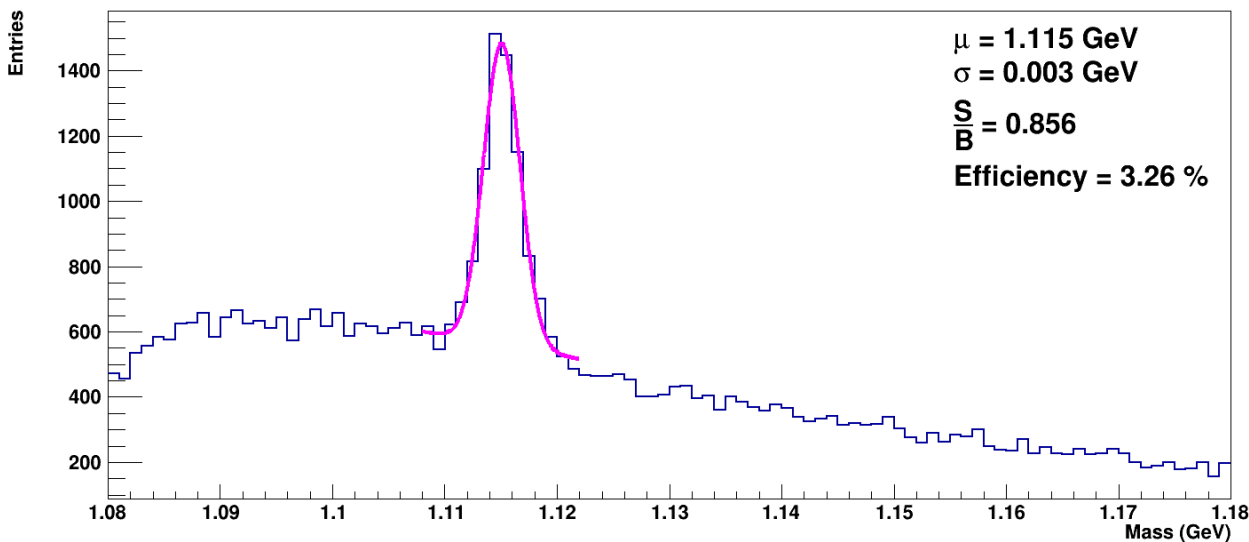
## Lambda hyperons



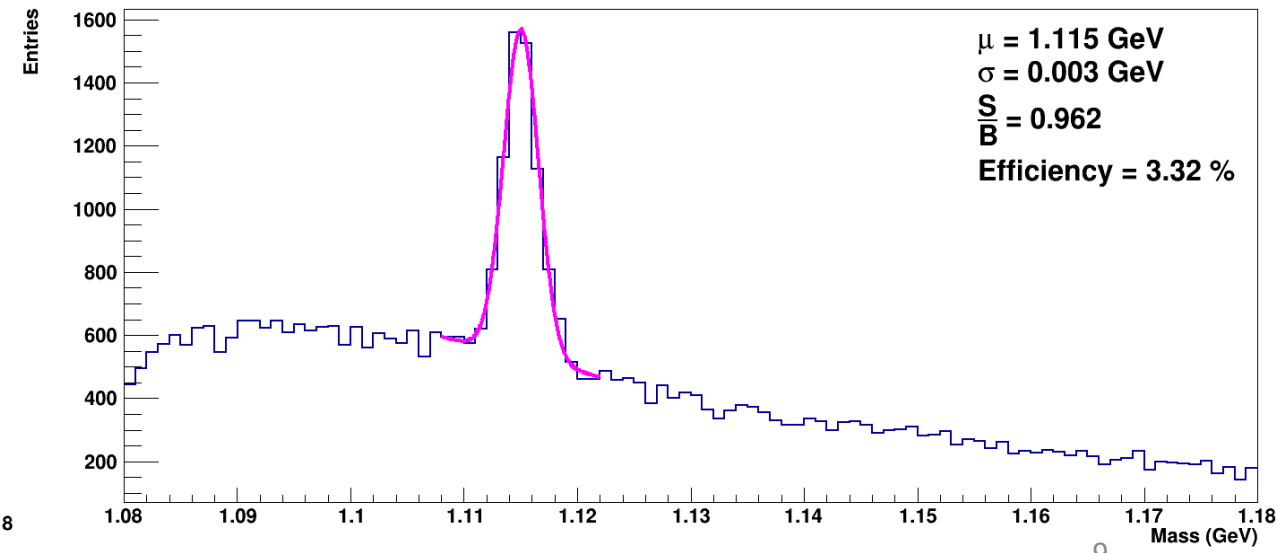
SiMD



BD



Beam blurring



Target

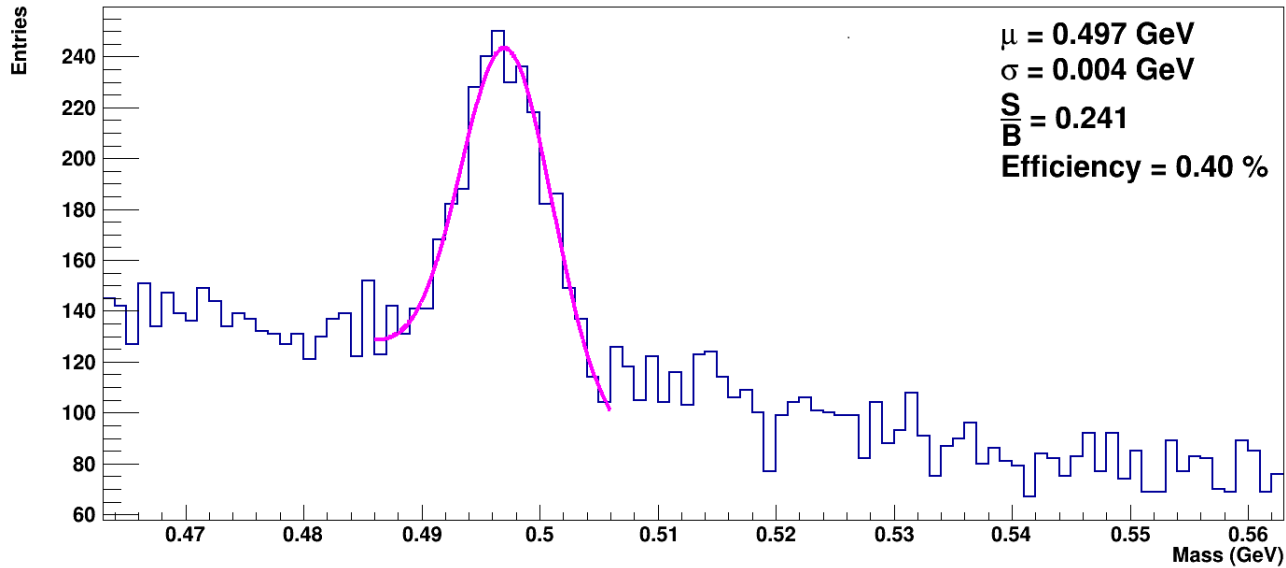
# Results

## Lambda hyperons

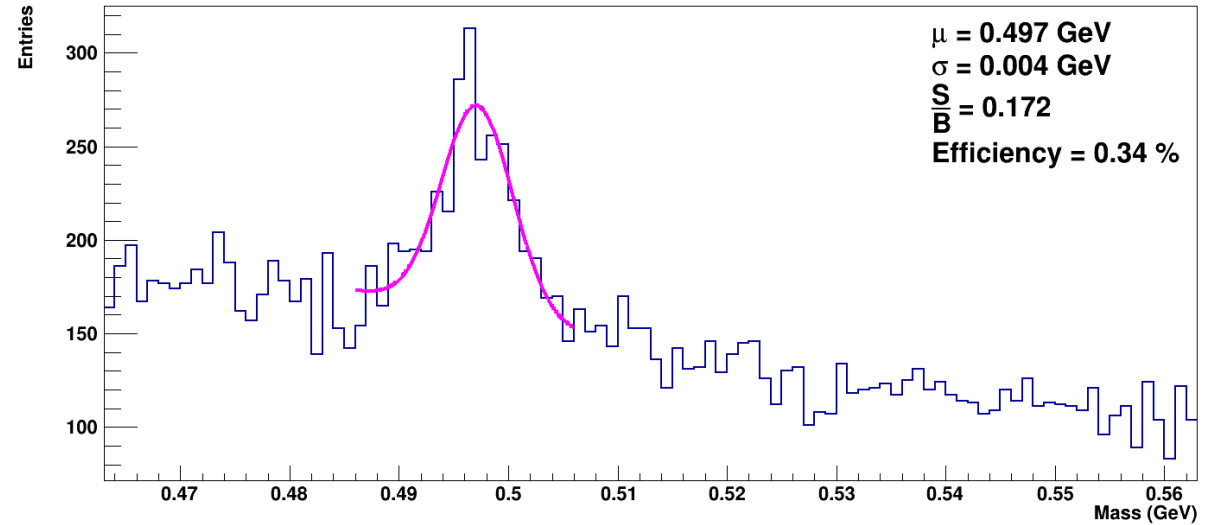
	Ideal case	SiMD, BD, target и размытие пучка	SiMD	BD	Target	Beam blurring
$\mu$ (GeV)	1.115	1.115	1.115	1.115	1.115	1.115
$\sigma$ (GeV)	0.003	0.003	0.003	0.003	0.003	0.003
S	3713	3466	3606	3720	3733	3480
B	3574	4353	3730	3588	3881	4067
S/B	1.039	0.796	0.967	1.037	0.962	0.856
Efficiency (%)	3.30	3.07	3.21	3.30	3.32	3.26

# Results

## $K_S^0$



Ideal case



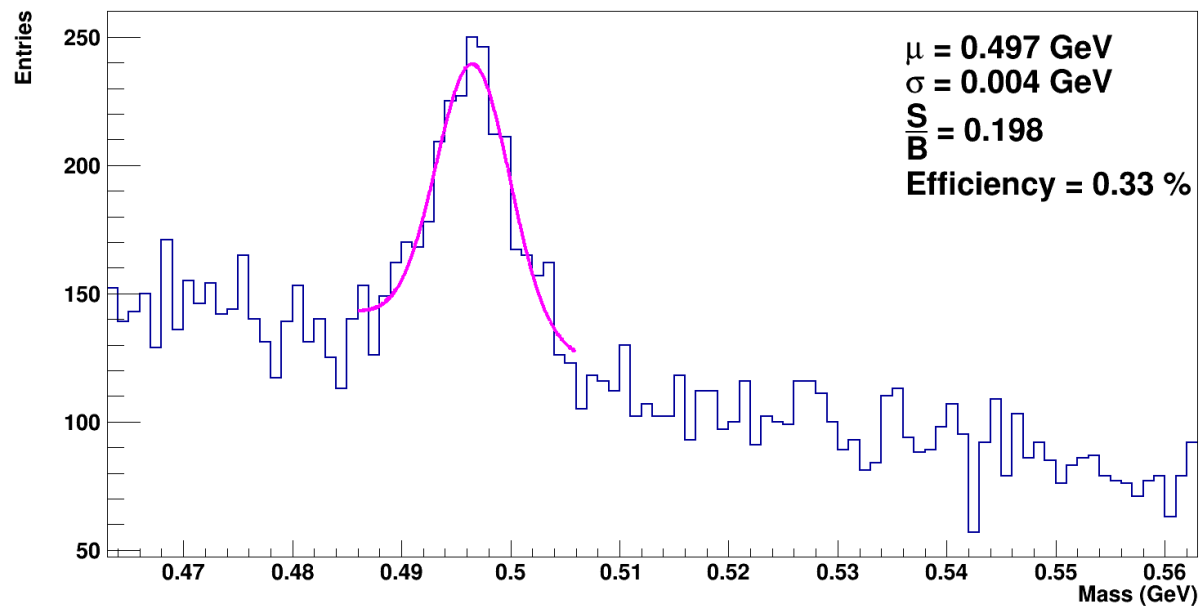
SiMD, BD, target and beam blurring

### Cuts

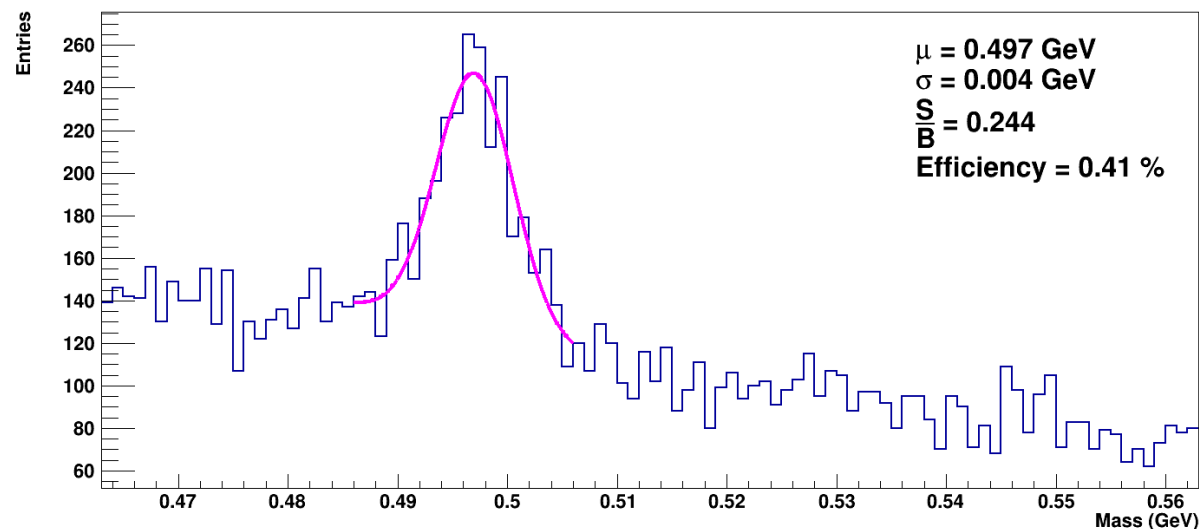
- $1.0 < \text{path} < 20$
- $0.0 < \text{DCA12} < 0.3$
- $0.0 < \text{DCA0} < 0.2$
- $0.2 < \text{DCA1} < 3.0$
- $0.2 < \text{DCA2} < 3.0$

# Results

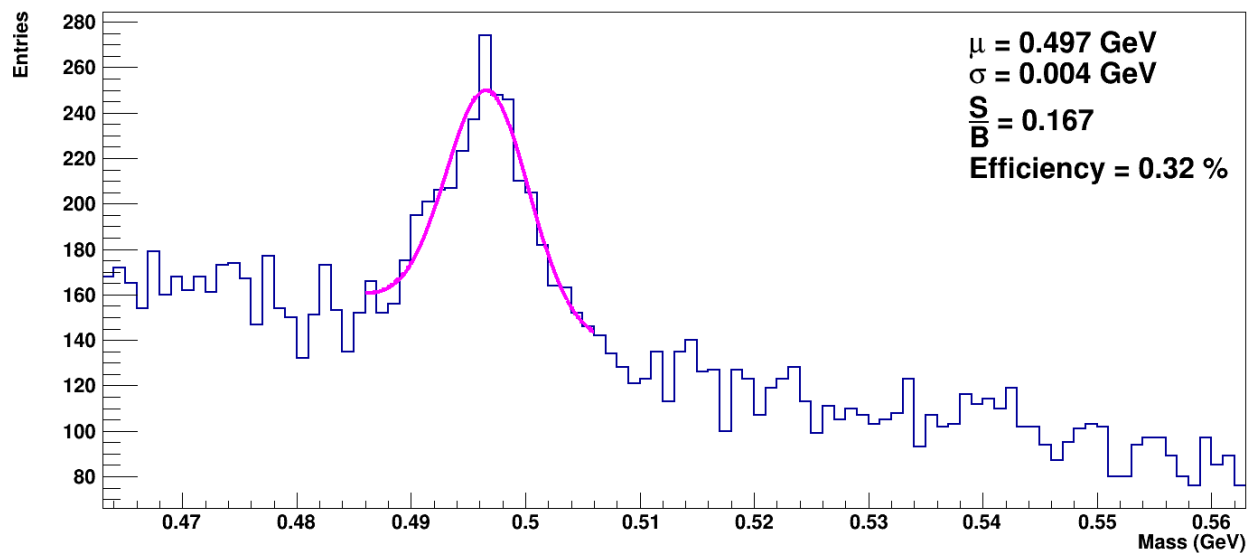
$K_S^0$



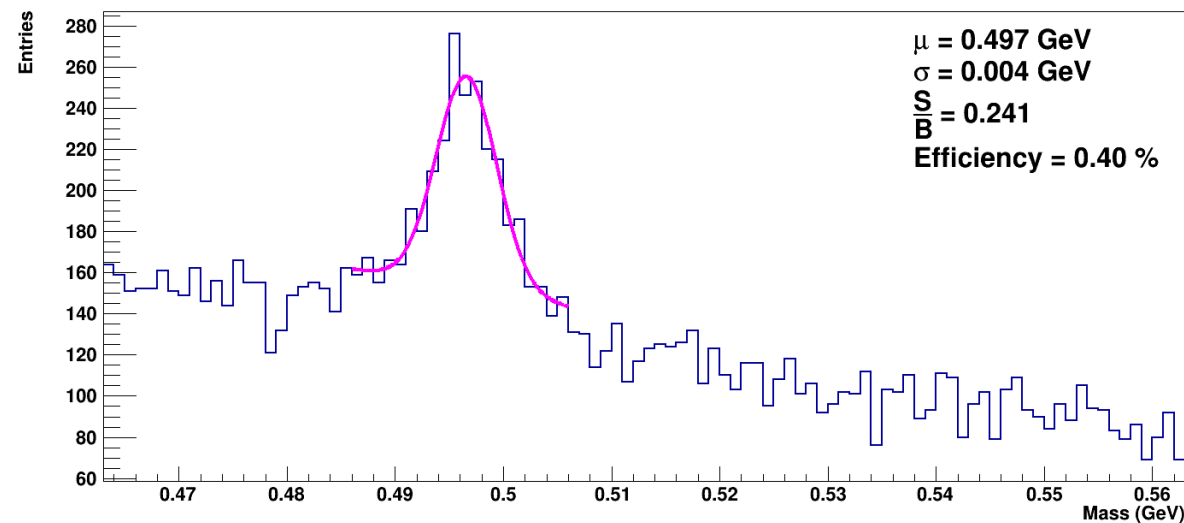
SiMD



BD



Beam blurring



Target

# Results

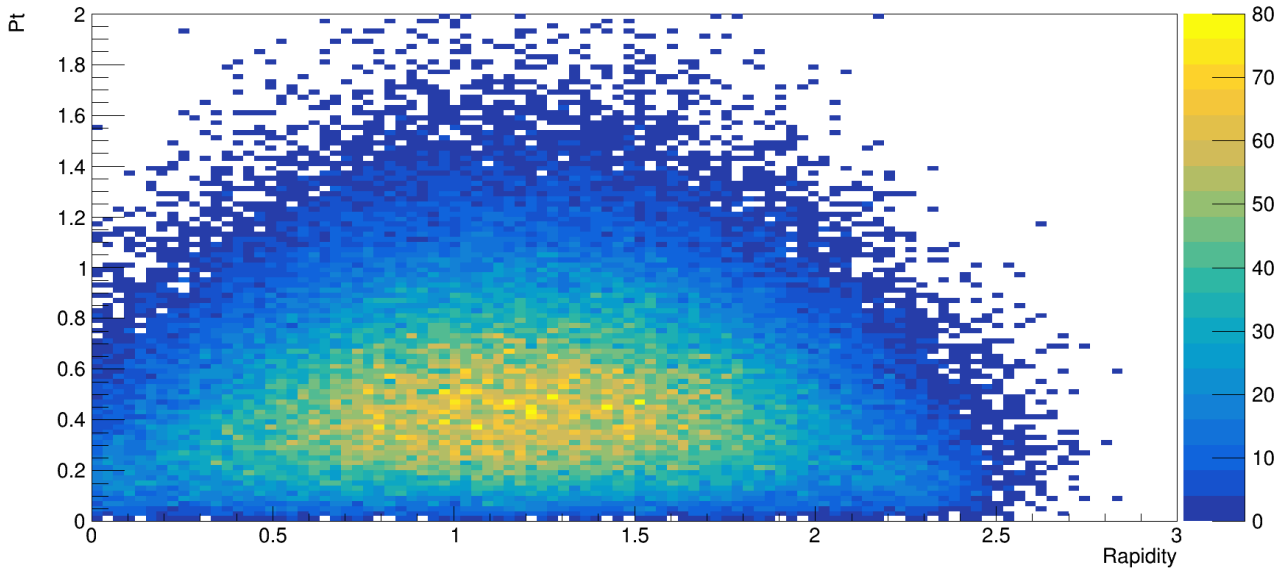
 $K_S^0$ 

	Ideal case	SiMD, BD, target и размытие пучка	SiMD	BD	Target	Beam blurring
$\mu$ (GeV)	0.497	0.497	0.497	0.497	0.497	0.497
$\sigma$ (GeV)	0.004	0.004	0.004	0.004	0.004	0.004
S	380	323	318	391	389	295
B	1574	1882	1607	1598	1617	1761
S/B	0.241	0.172	0.198	0.244	0.241	0.167
Efficiency (%)	0.40	0.34	0.33	0.41	0.40	0.32

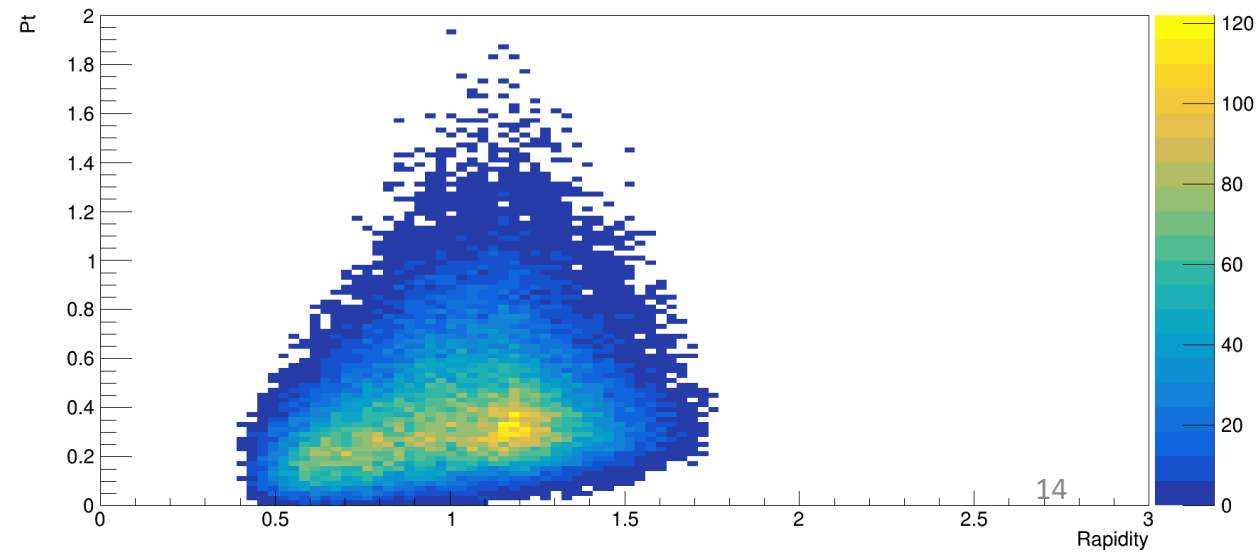
# Results

## Lambda hyperons

Pt vs rapidity lambda's after simulation



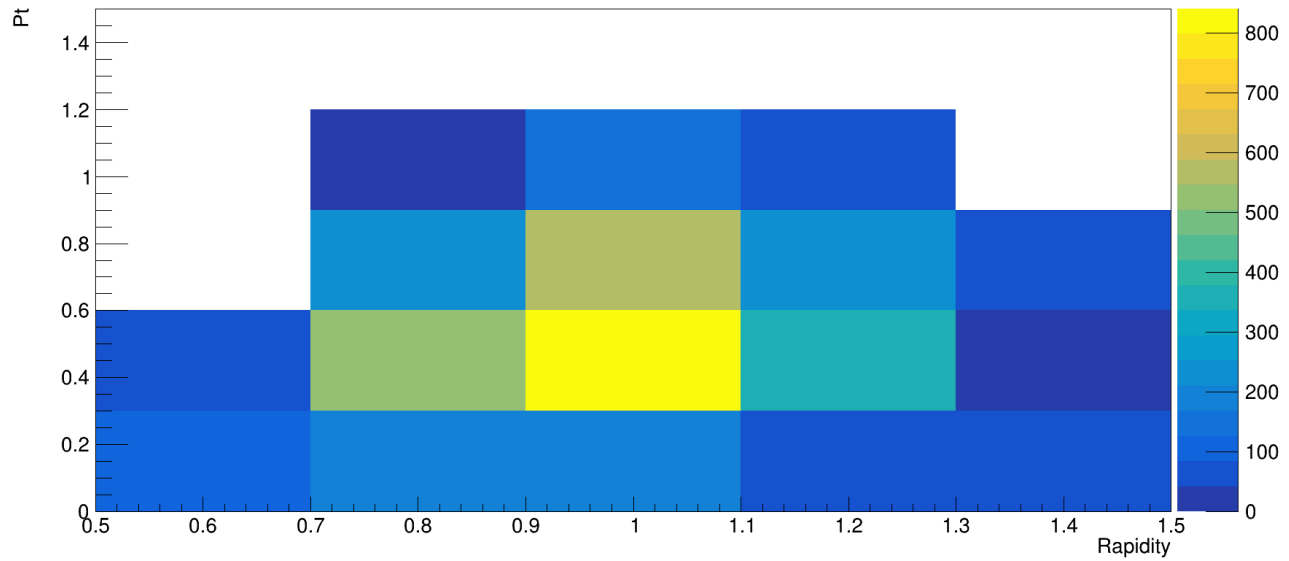
Pt vs rapidity lambda's after reconstruction



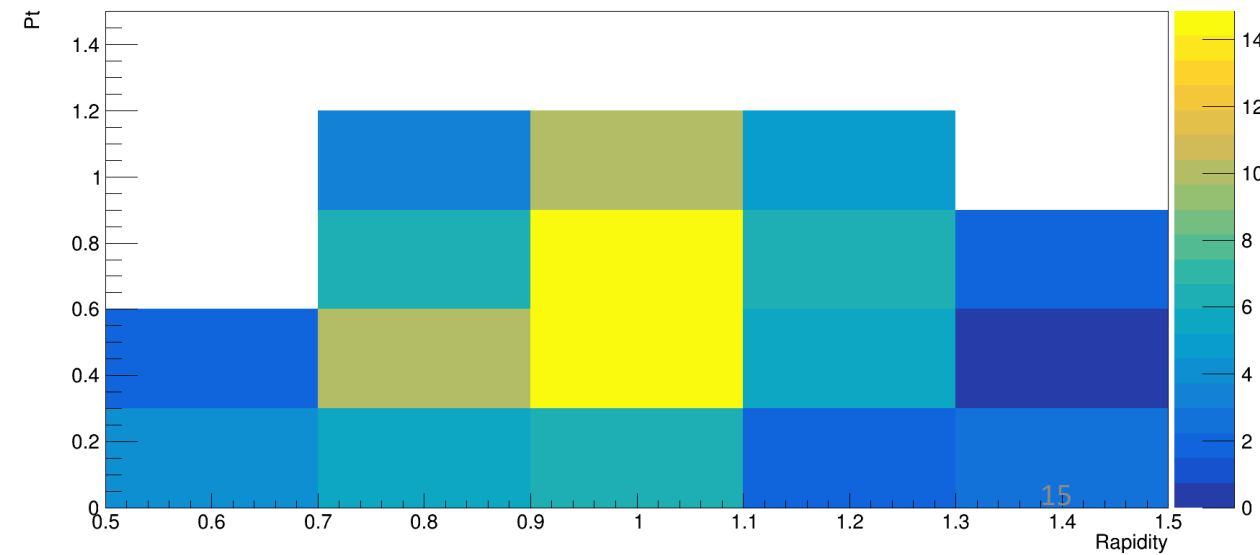
# Results

## Lambda hyperons

Pt vs rapidity lambda's after reconstruction and signal extraction



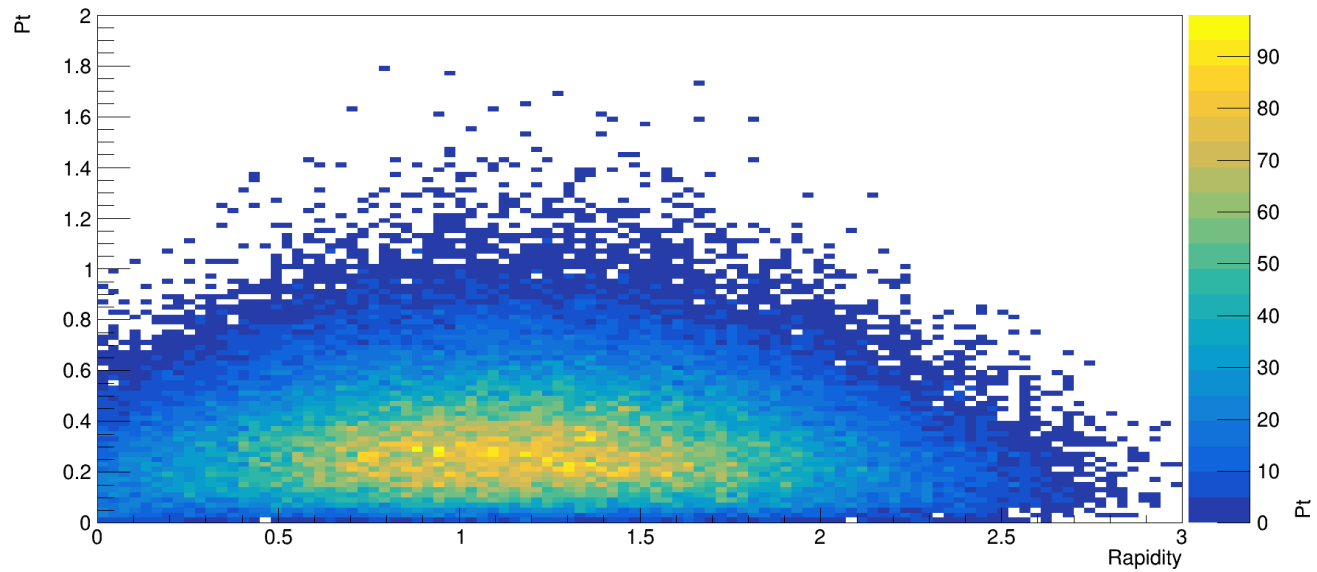
Efficiency lambda's depending on rapidity and Pt



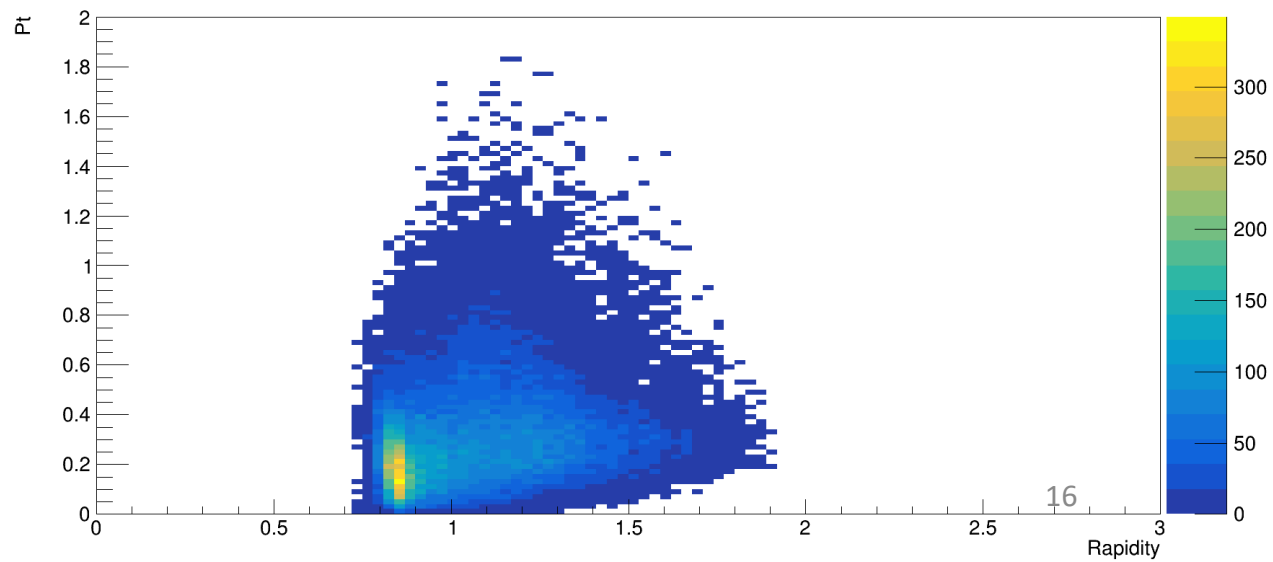
# Results

## $K_S^0$

Pt vs rapidity kaon's after simulation



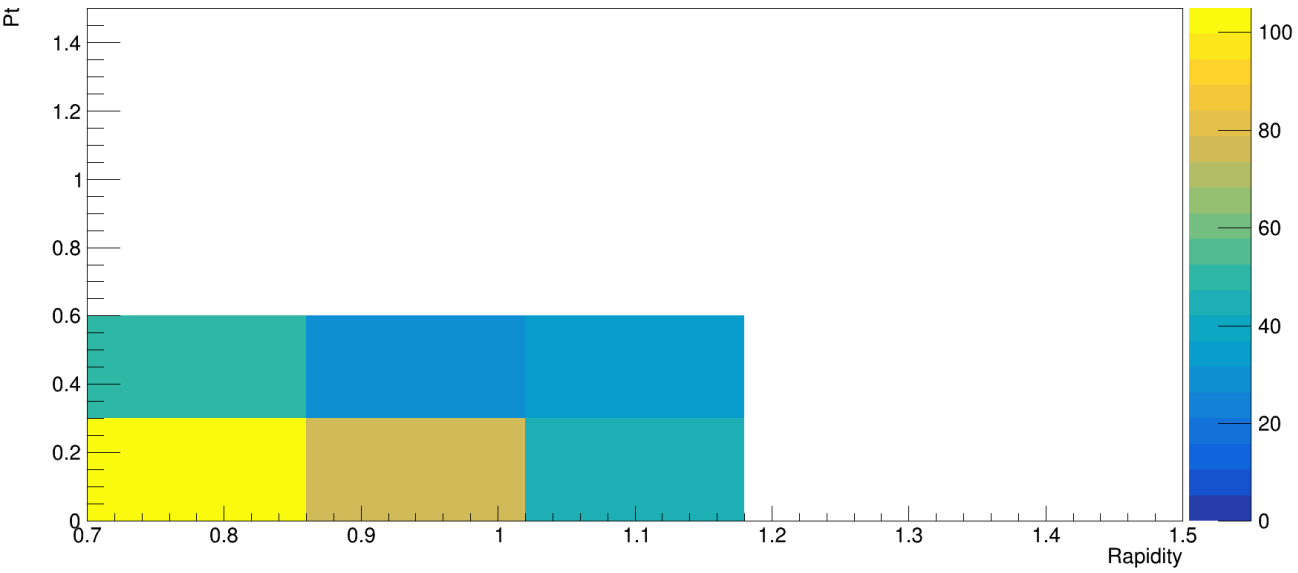
Pt vs rapidity kaon's after reconstruction and application of the cuts



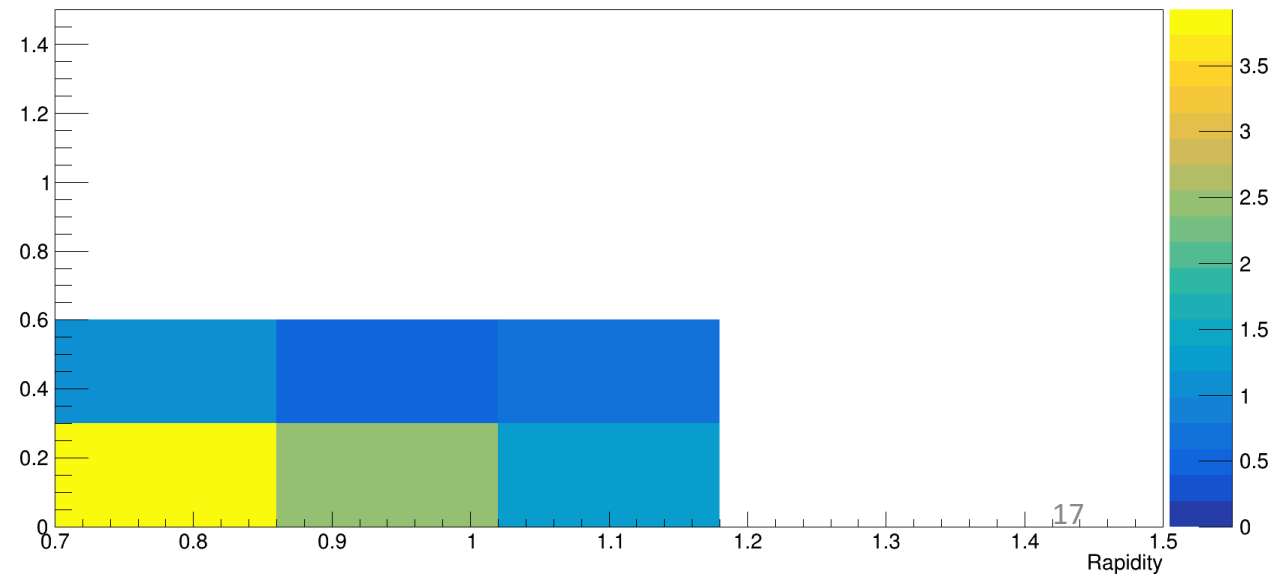
# Results

## $K_S^0$

Pt vs rapidity kaon's after reconstruction and signal extraction



Efficiency kaon's depending on rapidity and Pt



# Conclusion

- Simulation and analysis of 100,000 events for the ideal case and cases with different sources of background increment were carried out.
- The presence of lambda hyperon and  $K_S^0$  were revealed in both cases.
- Analysis of the influence of each source of background increment was carried out individually on 100,000 events.
- Efficiency depending on rapidity and transverse momentum and on both was derived for lambda hyperons and kaons.

# Future work

- Study of the effects of rotating the silicon stations by a certain angle on the recovery of strange particles.
- Verification of the algorithm on experimental data.

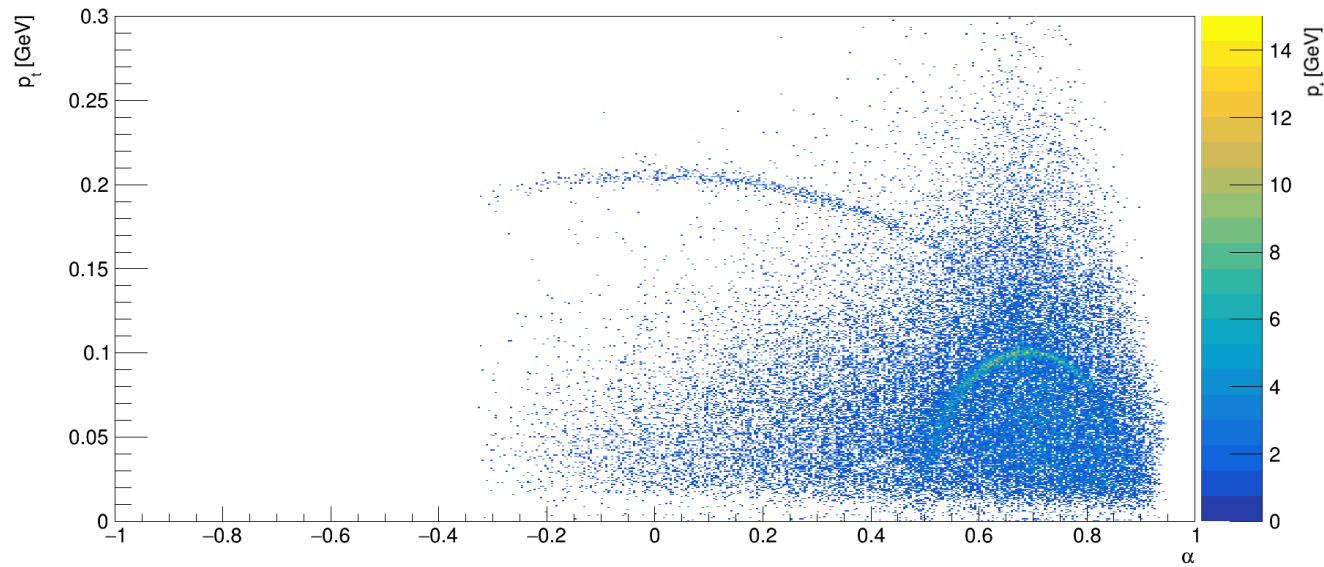
Thank you for your  
attention!

# Backup

# Results

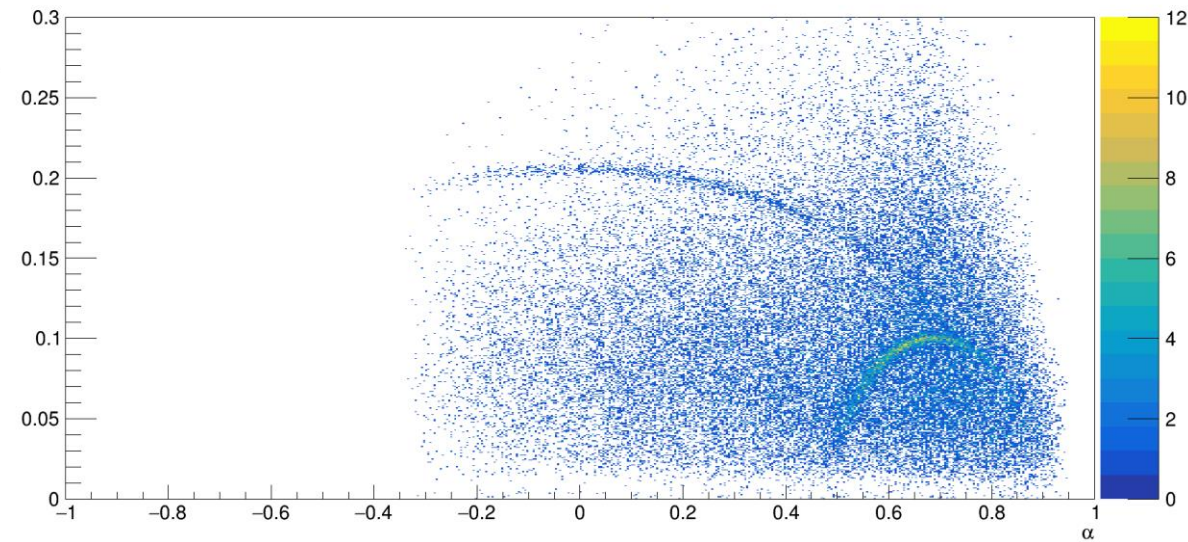
## Armenteros-Podolanski plots

Armenteros-Podolanski plot



Algorithm for lambda hyperon reconstruction

Armenteros-Podolanski plot

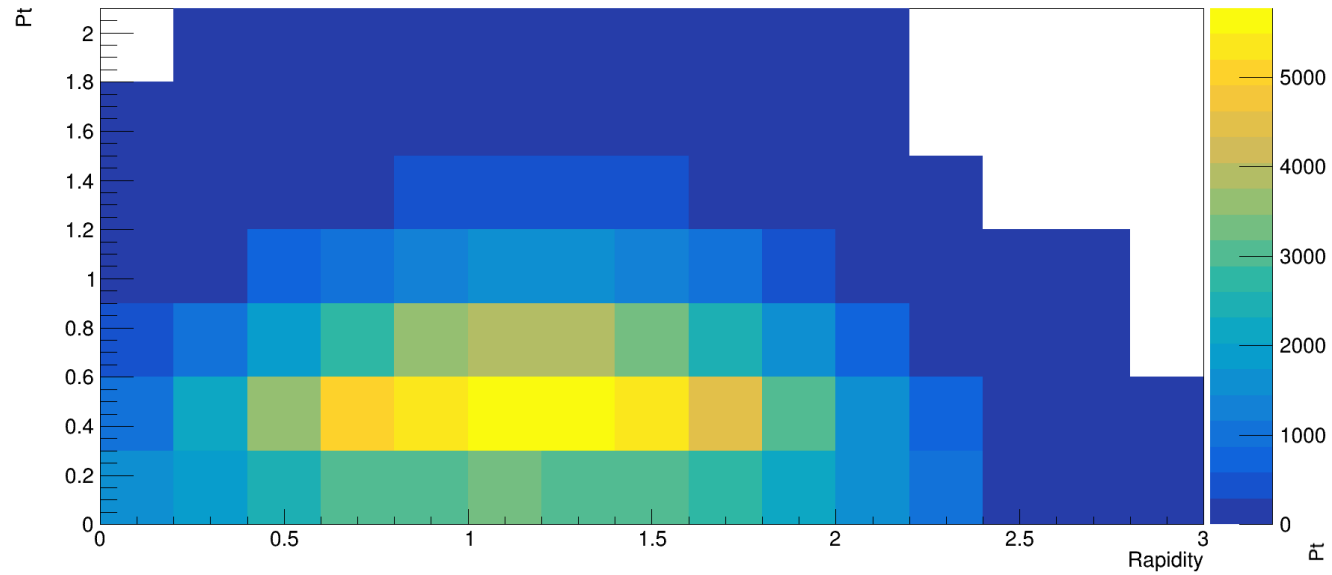


Algorithm for  $K_S^0$  reconstruction

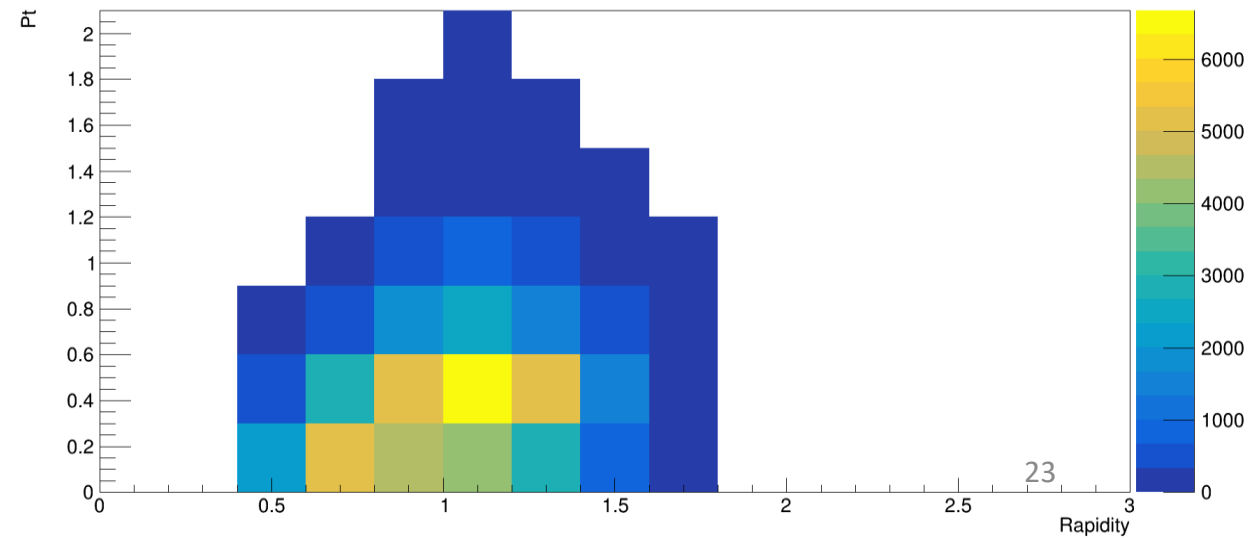
# Results

## Lambda hyperons

Pt vs rapidity lambda's after simulation



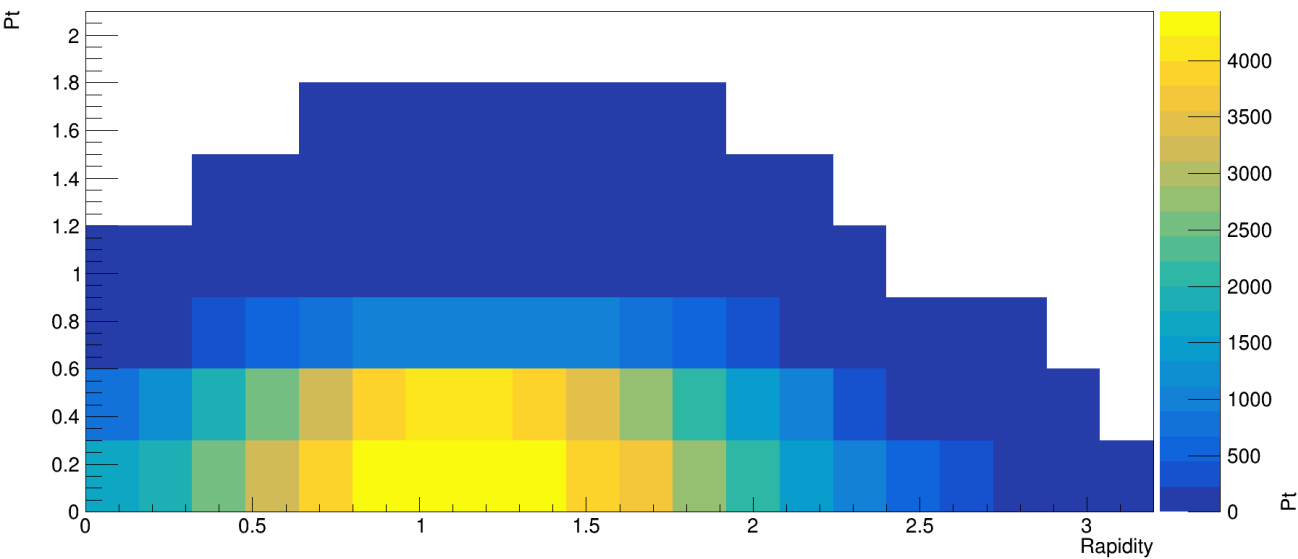
Pt vs rapidity lambda's after reconstruction



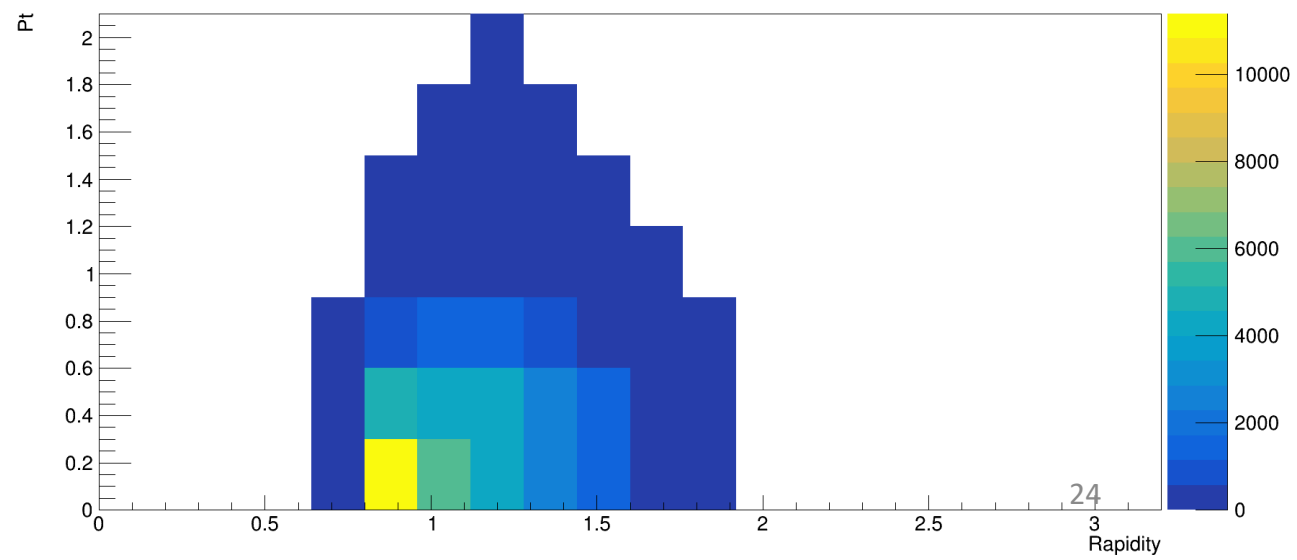
# Results

## $K_S^0$

Pt vs rapidity kaon's after simulation

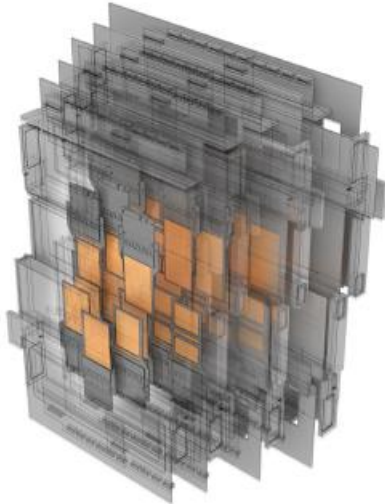


Pt vs rapidity kaon's after reconstruction and application of the cuts

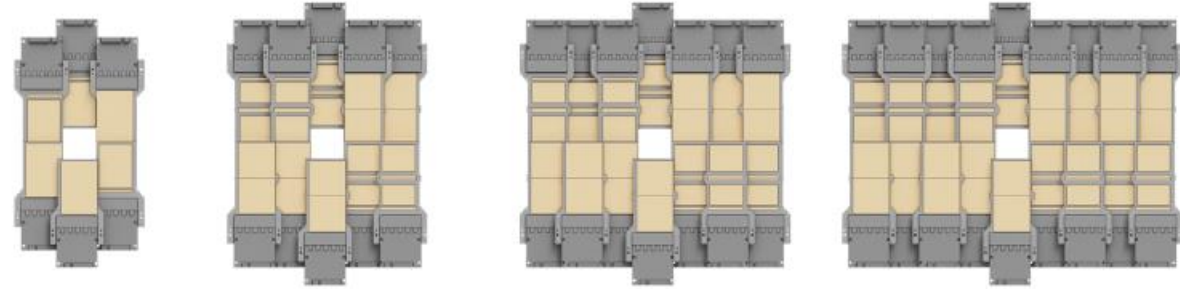


# Forward Silicon Detector

**Forward Silicon Detector (FSD)** is a high-precision coordinate detector of the inner tracking system of the BM@N setup. It consists of a set of silicon modules which are assembled into 4 stations.

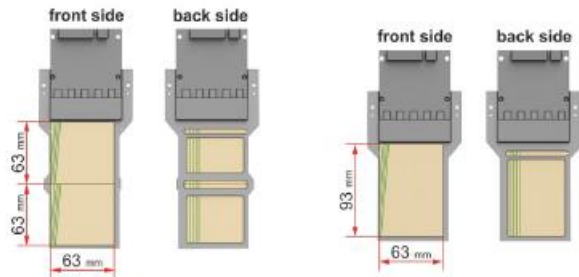


## Silicon stations



**Station 1:** 6 modules of  $63 \times 93 \text{ mm}^2$      **Station 2:** 10 modules of  $63 \times 126 \text{ mm}^2$   
**Station 3:** 14 modules of  $63 \times 126 \text{ mm}^2$      **Station 4:** 14 modules of  $63 \times 126 \text{ mm}^2$

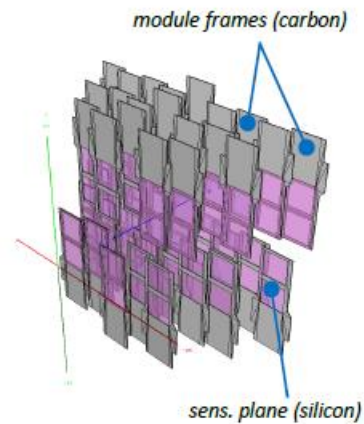
## Silicon module types



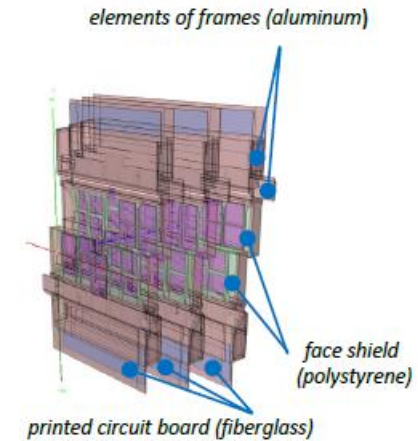
**Si-module with two double-sided strip sensors of  $63 \times 63 \text{ mm}^2$  each**     **Si-module with one double-sided strip sensor of  $63 \times 93 \text{ mm}^2$**

sensor thickness:  $300 \mu\text{m}$   
 strip pitch:  $\approx 100 \mu\text{m}$   
 stereo angle between strips:  $2.5^\circ$

## ROOT geometry



Basic ROOT geometry of the FSD detector



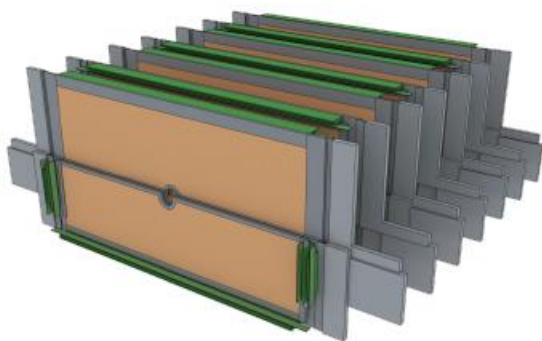
Detailed ROOT geometry of the FSD detector

Adding passive elements to the geometry allows us to take into account detector materials which affect the passage of particles through matter. This, in turn, improves the accuracy of the Monte-Carlo simulation.

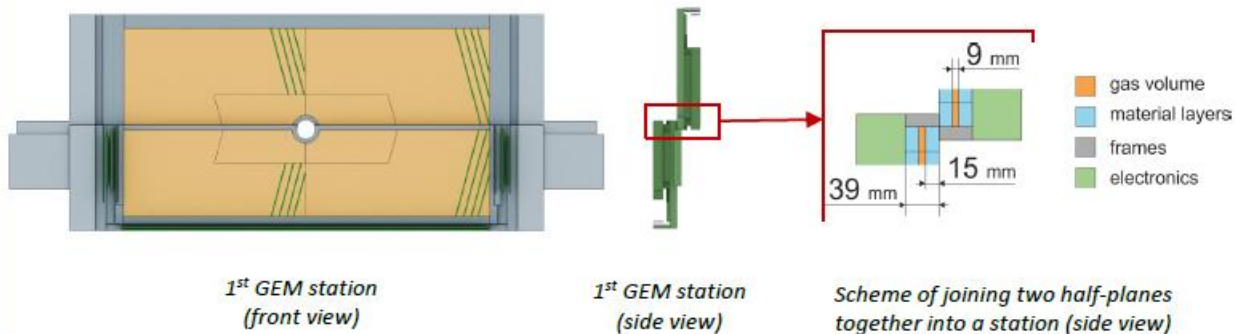
# GEM detector

**GEM (Gas Electron Multipliers)** is a microstrip coordinate detector of the central tracker in the BM@N setup. It consists of gaseous chambers with electron multiplier system inside.

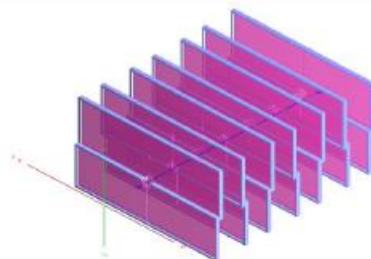
The configuration of this detectors for RUN-8 comprises **seven stations** located inside the magnet along the beam axis.



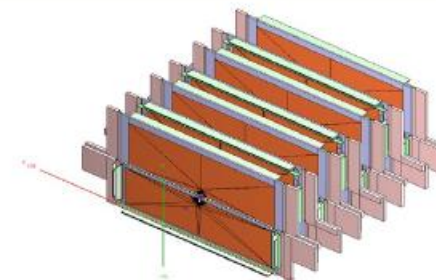
## GEM station assembly



## ROOT geometry

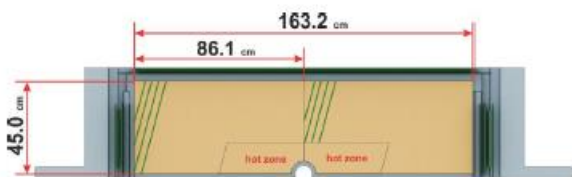


Basic ROOT geometry of the GEM detector

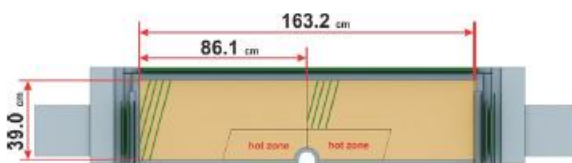


Detailed ROOT geometry of the GEM detector

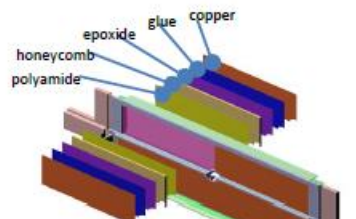
## GEM chamber types



Upper half-plane



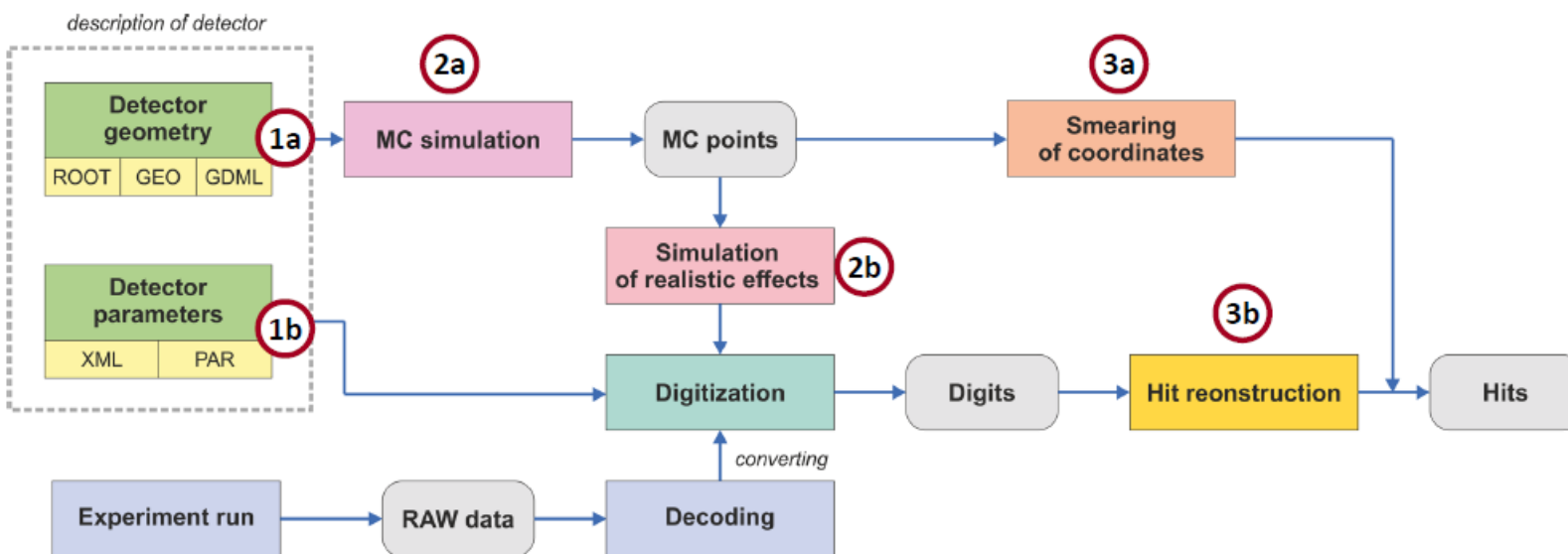
Lower half-plane



Sensitive area of a GEM chamber

Each active zone in a GEM chamber has a multi-layer structure. A layer has the following properties: thickness, material type and other characteristics which are taken into account in the Monte-Carlo simulation.

# Tracking detectors: software for data processing

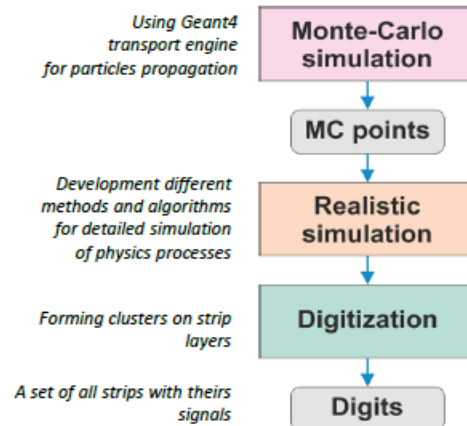


Basic stages of data processing for tracking detectors in BmnRoot

## Stages of data processing

1. **Complete description of a detector:**
  - a) Description of detector geometry (ROOT files)
  - b) Description of detector parameters (XML files)
2. **Simulation:**
  - a) Monte-Carlo simulation
  - b) Simulation of realistic effects
3. **Procedures of getting "hits" (Hit-reconstruction):**
  - a) Smearing Monte-Carlo points (hit producing)
  - b) Hit reconstruction from "digits":
    - Realistic simulation + digitization
    - RAW experimental data + digitization

## Realistic simulation steps



**Complete simulation** for detectors comprises the following stages:

1. Monte-Carlo simulation (getting MC-points by using Geant4)
2. Realistic simulation (taking into account the signal formation features)
3. "Digitization" (forming 'digits' as signal on the strips)